Engineering and Technology Journal
Journal homepage: https://etj.uotechnology.edu.iq

Effect of Different Parameters on Raman Scattering Released from Nb_2O_5 Nanostructures Prepared via PLD Technique

Suhair R. Shafeeq[a], Evan T. Salim[b*], Mohammed J.AbdulRazzaq[a], M. H. A. Wahid[c]

[a] Laser and Optoelectronic Engineering Dept., University of Technology-Iraq, Alsina'a street, 10066 Baghdad, Iraq.
[b] Applied Science Dept., University of Technology-Iraq, Alsina'a street, 10066 Baghdad, Iraq.
[c] Semiconductor Photonics & Integrated Lightwave Systems (SPILS), School of Microelectronic Engineering, University Malaysia Perlis, 02600, Arau, Perlis, Malaysia.
*Corresponding author Email: mailto:loe.21.14@uotechnology.edu.iq

HIGHLIGHTS

- T-Nb_2O_5 nanoparticle was achieved.
- A single step of laser ablation in liquid at different preparation parameters was performed.
- Raman spectroscopy and structural properties were conducted and analyzed.

ARTICLE INFO

Handling editor: Makram A. Fakhri

Keywords:
Pulsed laser deposition
Octahedron
optimized
Raman scattering
orthorhombic

ABSTRACT

Due to the significance of Nb_2O_5 as a promising industrial and biomedical material and the importance of Raman analyses to identify nanostructural molecular responsivity for various applications, this study aims to investigate Nb_2O_5 molecular bands that emerged under the impact of the Raman scattering phenomenon. Besides other advantages, Raman scattering analyses can provide a further investigation of the nanostructural polycrystalline phases supporting the XRD analyses. A pulsed laser was selected as the deposition technique for Nb_2O_5 thin films prepared with four different parameters. The selection of the pulsed laser deposition (PLD) method was due to the insufficient studies and investigations of Nb_2O_5 nanostructures prepared via this method. The deposition parameters included the laser energy per pulse, substrate temperature, laser wavelength, and the number of laser pulses. Each preparation parameter was studied in a range, and one obtained value was optimized or selected for investigating the next parameter. Q-switched Nd:YAG pulsed laser was employed for this purpose. Orthorhombic (T-Nb_2O_5) and monoclinic (H-Nb_2O_5) were obtained and investigated. XRD analysis was incorporated to confirm the resulting Nb_2O_5 phases. Previous studies and observations of Niobium (V) oxide molecular Raman scattering bands were also listed for comparison purposes. The results of this study were well-agreed with the previously obtained results.

1. Introduction

Niobium pentoxide (Nb_2O_5) is considered an n-type semiconductor with about 15 structural phases. Nb_2O_5 has high air stability, water insolubility, and anti-corrosion features that qualify it as a promising candidate for various applications. The reported optical band gaps ranged from 3.1 to 5.3 eV[1]. Catalysts, biosensors, and electrochromism are the common applications of Nb_2O_5[2-3]. Nb_2O_5 is also popular in solar cells, batteries, memristors, dental implant anti-corrosion coating, anti-toxic nanocoating, and other industrial and biomedical applications[4-6].

The pulsed laser deposition (PLD) technique is one of the physical vapor deposition methods (PVD) that successfully demonstrated nanostructure growth. PLD can be used to prepare different nanomaterials and nanostructures by a pulsed laser bombardment of a target material in the form of a solid pressed pellet. Thin film preparation can be readily obtained by this method. Moreover, the prepared film can be well-organized with a desirable quality for various applications [7].

Raman scattering is a non-destructive technique to identify the structural properties related to the obtained crystal phases and lattice defects, including external strains and molecular bonds. Individual layers of thin films can also be investigated since Raman scattering provides the superposition of the spectra arising from the lattice vibrations. In addition, very small nanoscale constituents can be detected as the lattice vibrations are sensitive to the neighborhood. In semiconductor compounds, concentrations of charge carriers and carrier scattering durations may also be resolved via Raman analyses [8-9]. The principle of Raman scattering impact on a molecule is illustrated in the Jablonski diagram, Figure 1, that includes Raman scattering phenomena.

http://doi.org/10.30684/etj.2022.134436.1238
Received 25 June 2022; Accepted 19 August 2022; Available online 23 September 2022
2412-0758/University of Technology-Iraq, Baghdad, Iraq

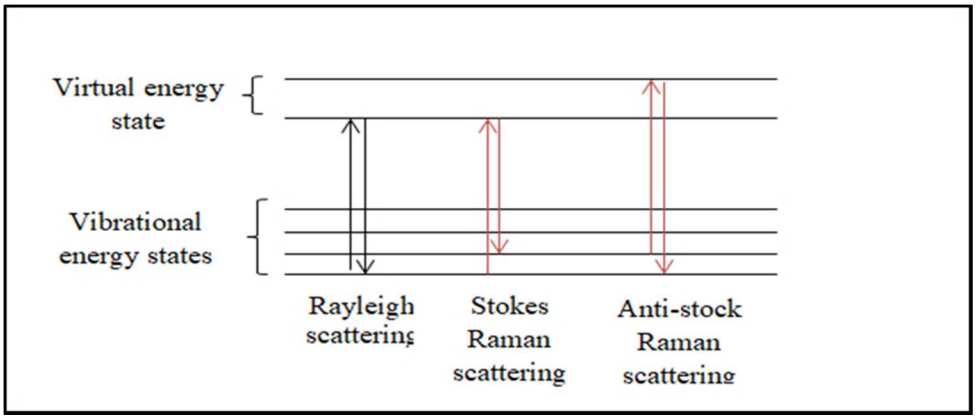

Figure 1: Jablonski diagram illustrating Raman scattering principle

Raman scattering phenomena occur in inelastic when monochromatic incident radiation and molecular vibrational states interact, resulting in inelastic collisions. Shifting in the scattered radiation can occur with stokes or anti-stokes shifting. In the case of stoke shifting, the scattered radiation frequency is less than the incident radiation frequency. In contrast, anti-stokes lines occur due to the higher scattered frequency than the incident frequency. Stoke shifting occurs in case the scattered photons of incident radiation appear in lower wavenumber regions because the scattered wavelength is higher than the incident wavelength. On the other hand, anti-stoke shifting is observed in higher wavenumber regions, which occur when the scattered wavelength is lower than the incident radiation wavelength. Polarization is changed when the molecule's vibrational states are exposed to the incident radiation of the monochromatic source [10,11]. As a result, various modes are observed in the molecular bonds. These modes are symmetric, asymmetric, and bending stretching of the molecule are illustrated in Figure 2 (a-b). In this study, Nb_2O_5, one of the prominent materials in biomedical and industrial applications, was prepared via pulsed laser deposition (PLD) technique and tested under the Raman scattering phenomenon.

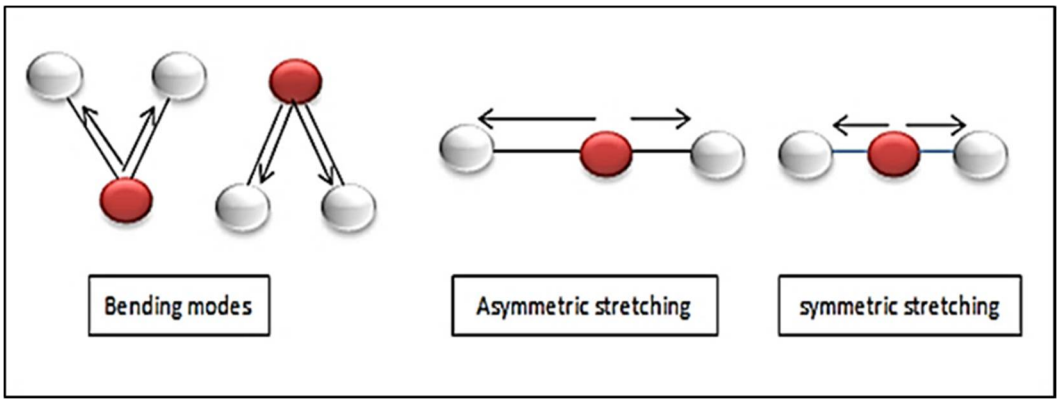

(A)

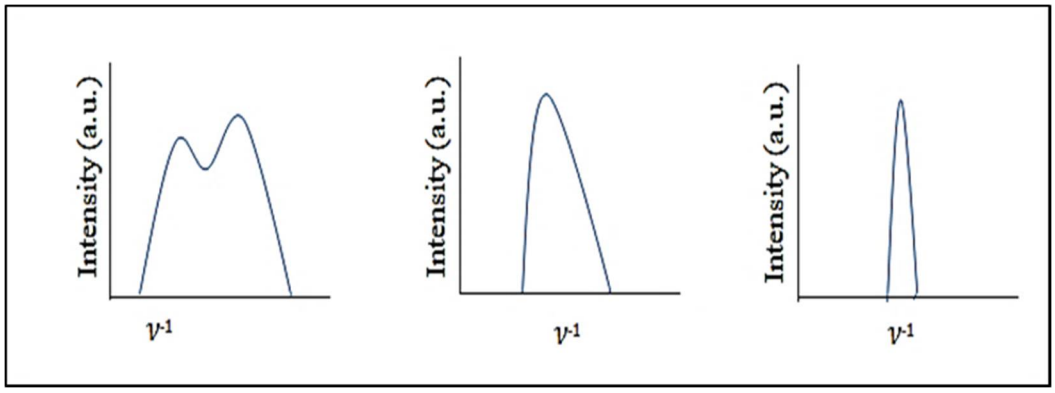

(B)

Figure 2: (a) Raman stretching and bending modes. (b) Raman intensity as a function of wavenumbers

2. Experimental Work

The selected substrates were quartz slides cut equally to (2 x 1 cm) to deposit Nb_2O_5 thin films onto them. The selected substrates were cleaned to remove impurities and to ensure producing contaminants-free niobium pentoxide thin films. A mixture of (30 ml) deionized water and (15 ml) ethanol was used with an ultrasonic device for the cleaning purposes of the experimental

tools. The cleaning process was continuous for about fifteen minutes. Niobium(V) oxide powder from Merck (Kenilworth, NJ) with (99.99%) purity was pressed under 12 tons' pressure to form a disk with a diameter of (2.5 cm) and a height of (0.5 cm). The experimental parameters of this study are planned as in Table 1. The selected deposition parameters were to provide a full investigation of Nb_2O_5 thin film molecular behavior under the Raman scattering mechanism. Laser pulse energies were from more than 400 mJ to lower than 700 mJ. The selection of pulse energy within this specific range was a result of using the fundamental wavelength (1064nm) of Q-switched Nd:YAG laser that possesses lower photon energy (1.16 eV) as compared with the second harmonic wavelength (2.33 eV). If lower pulse energy was selected, thermal shockwaves might lead to droplets or particulates on Nb_2O_5 as a normal consequence of the pulsed laser deposition (PLD) technique. These would degrade the thin film stoichiometry and might result in distorted Raman scatterings. As for the substrate temperature, the chosen temperatures were 350, 450, and 550 °C to ensure the adhesion process of Nb_2O_5 nanoparticles on the substrates and for depositing well-organized layers of the thin film by exploiting the temperature factor as it plays a crucial role in crystallization. Nb_2O_5 thin film prepared by the second harmonic wavelength (532nm) of the Q-switched Nd:YAG laser was employed for comparative purposes of Nb_2O_5 thin films behaviors under the Raman scattering phenomenon (shorter wavelength with higher photon energy generally leads to a smaller particle size that effects on thin film thickness structures, thus responsivity to incident radiation in Raman spectroscopy). Eventually, the number of laser shots differed with 100, 200, and 300 pulses to investigate the thickness impact on the scattering process induced by Raman. The PLD system employed for Nb_2O_5 thin film preparation is shown in Figure 3.

Table 1: Various deposition conditions employed to synthesize Nb_2O_5 by PLD

Conditions	Changed parameters	Fixed parameters
Laser beam energy	422 mJ 551 mJ 657 mJ	λ= 1064 nm Substrate temperature= 350 °C Number of pulses=200
Substrate temperature	350 °C 450 °C 550 °C	λ= 1064 nm Energy per pulse =657 mJ Number of pulses=200
Wavelength	1064 nm, 532 nm	Energy per pulse=657 mJ Substrate temperature= 350 °C Number of pulses=200
Number of pulses	200 300 400	λ= 1064 nm Energy per pulse=657 mJ Substrate temperature= 350 °C

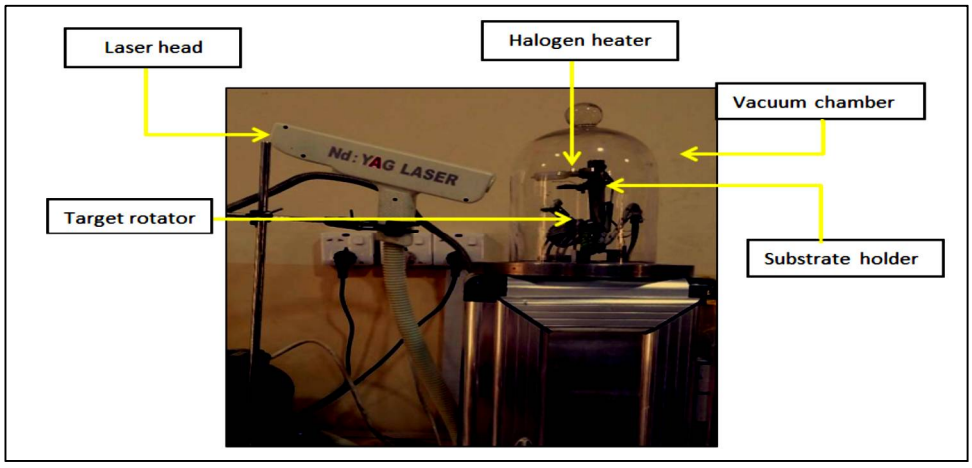

Figure 3: Pulsed laser deposition system used for Nb_2O_5 thin films preparation

Raman spectrometer from sunshine (version V2-86) was used to provide a further study of Nb_2O_5 structures and molecular behavior. The parameters used in Raman analyses are listed in Table 2.

Table 2: Raman parameters were used to test Nb_2O_5 thin films scattering pattern

Testing parameters	Testing values
Monochromatic source	Nd:YVO4 solid-state laser
Radiation wavelength	532 nm generated by KTP crystal
Beam diameter at the aperture	0.70 mm
Beam divergence	<1.5 mrad.
Operation mode	TEM00

To understand Raman scattering phenomena by Niobum(V) oxide thin films, the incident laser source frequency is obtained from the following well-known formula [12-15]:

$$c = \lambda f \quad (1)$$

Where (c) is the speed of the light in space (3 x 10^8 m/s), (λ) is the monochromatic laser source wavelength (m), and (f) is the monochromatic laser source frequency (Hz). Then, the obtained frequency was calculated in terms of wavenumber to compare with the obtained Nb_2O_5 Raman wavenumbers.

3. Results and Discussion

3.1 Laser Energy Impact

NbO_6 octahedron is the major constituent of the amorphous or polycrystalline phases of Nb_2O_5 [6]. The most common crystal phases, among 15 discovered phases, are pseudohexagonal (TT-Nb_2O_5), orthorhombic (T-Nb_2O_5), and monoclinic (H-Nb_2O_5) [16]. The Nb atoms in the T-Nb_2O_5 phase structure are commonly surrounded by six O atoms in the ab-plane. In the monoclinic phase, H-Nb_2O_5 with octahedral unit cells are linked by the corner-shared block [17]. T-Nb_2O_5 and H-Nb_2O_5 are illustrated in Figure 4. T-Nb_2O_5 and H-Nb_2O_5 vibrational modes and their related wavenumber regions were commonly observed by other authors, as listed in Table 3.

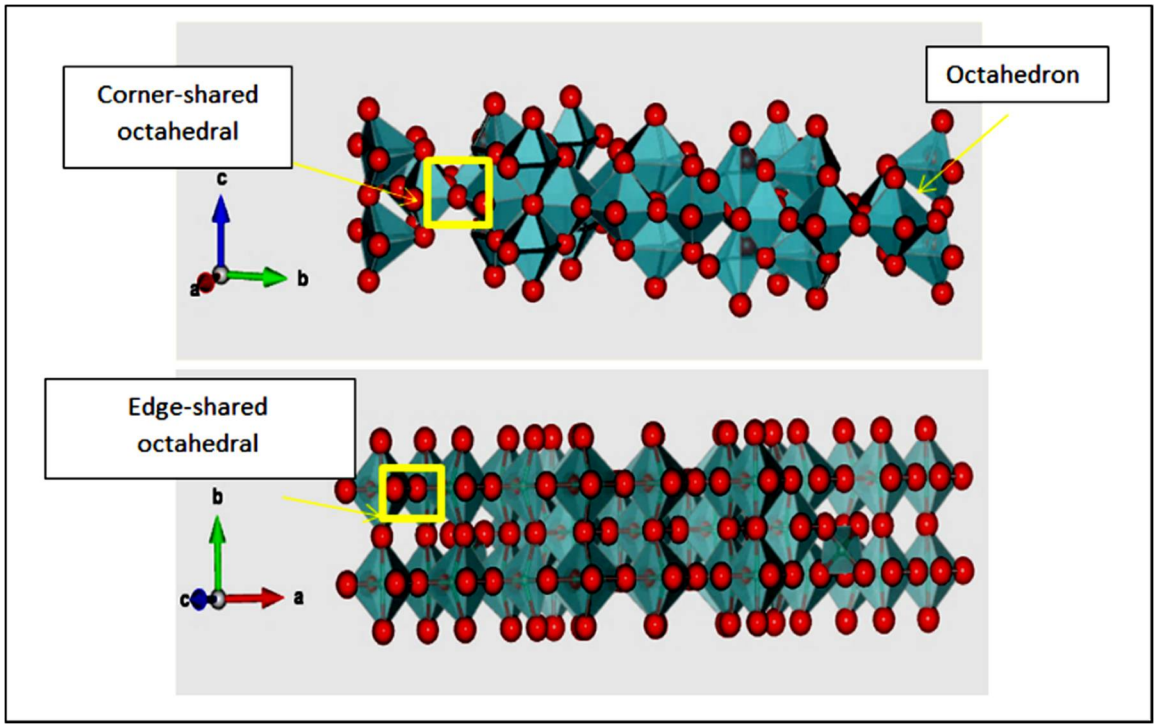

Figure 4: T-Nb_2O_5 (upper) with corner-shared octahedral. (b) H-Nb_2O_5 (bottom) with corner-shared octahedral

Table 3: T-Nb_2O_5 and H-Nb_2O_5 molecular bending and stretching observed modes by some authors [14-17]

band wavenumber (cm^{-1})	Vibrational mode	Nb_2O_5 structural phase	Ref.
204-549	Bending	H-Nb_2O_5	[18]
112, 122, 230, 257, 299, 545, 622, 649, 893, 834	Bending	H-Nb_2O_5	[19]
307,345,394, 470, 549, 613, 627, 663, 674, 760, 820, 843, 898, 993	Symmetric	H-Nb_2O_5	[20]
241, 688	Bridging bond	T-Nb_2O_5	[19]
192, 327, 308,465, 689,809	Bending and stretching	T-Nb_2O_5	[21]

Figure 5 shows the Raman spectra of the obtained thin films prepared by different Q-switched Nd:YAG pulsed laser energies. The tested samples were in the range of 0 to 1100 cm^{-1}. Since the laser source wavenumber is (18797 cm^{-1}) calculated from Equation 1, all the obtained results showed Raman stoke-shifting (the frequency is inversely proportional to the wavelength by the speed of light as the proportion constant). Below 400.6 cm^{-1}, peaks with high intensities were observed. These peaks are called the NbO_6 octahedral bending modes [19,21]. Around 600 cm^{-1}, stretching modes were observed, and the ref obtained a similar range [18]. The observed bands after 1000 cm^{-1} were assigned for the edge-shared octahedra. The band centered at 642.3 cm^{-1} was T-Nb_2O_5 for the film synthesized at 657 mJ. At 990.2 cm^{-1}, H-Nb_2O_5 intense broadened band was observed [20]. Other bands weakly appeared at abound 460.1 cm^{-1} referring to the framework vibration of oxygen metal oxide structures. A very close indication was in ref [22]. The observed broadening in Raman bands can be attributed to the phonon linewidth modes as a function of temperature, besides other parameters, including the thermal expansion and the strain caused by the lattice mismatch. These observations were similarly found in[23]. The bands below 400.6 cm^{-1} emerged with high intensities that increased with the laser energy. That can be assigned for the compression of the material molecules. This compression caused an increase in the

intensities and a slight reduction in the linewidths. This behavior was similarly indicated by ref [18]. The observed broadening in Raman bands can be attributed to the phonon linewidth modes as a function of temperature, besides other parameters, including the thermal expansion and the strain caused by the lattice mismatch. These observations were similarly found in [23]. The bands below 400.6 cm^{-1} emerged with high intensities that increased with the laser energy. That can be assigned for the compression of the material molecules. This compression caused an increase in the intensities and a slight reduction in the linewidths. This behavior was similarly indicated by ref [18]. Nb_2O_5 thin film prepared at 657 mJ was selected to study the substrate temperature for further investigations.

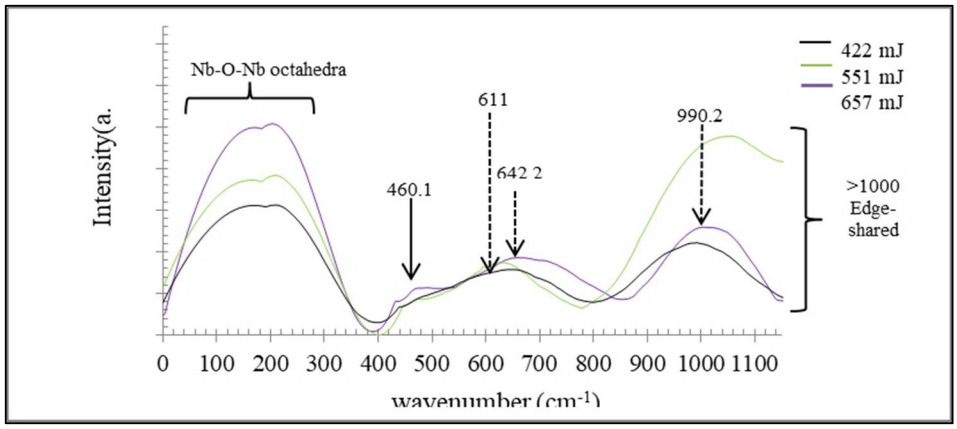

Figure 5: Raman spectra for Nb_2O_5 prepared films by Nd:YAG at different pulse energies

3.2 Substrate Temperature Impact

The substrate temperature was elevated from 350 °C to 550 °C with an increment scale of 100 °C. Raman scattering for the prepared Nb_2O_5 thin films at different substrate temperatures is illustrated in Figure 6. The octahedral stretched vibrational modes of prepared films were below 100 cm^{-1} for 450 and 550 °C. The band that appeared at 383.1 cm^{-1} was indicated for the Nb-O-Nb deformed angle. A similar assignment was found in ref [24]. Nb_2O_5 thin films synthesized on a substrate with a temperature of 550 °C were slightly observed in a higher wavenumber value. The orthorhombic (T-Nb_2O_5) asymmetric stretched modes for the films deposited on substrates with temperatures of 350, 450, and 550 °C were observed at 642.2, 662.7, and 679.6 cm^{-1}, respectively[18-20]. The bands that emerged at around 760.2 cm^{-1} were assigned for the monoclinic (H-Nb_2O_5). Other bands for monoclinic (H-Nb_2O_5) appeared in the region that exceeded 900 cm^{-1}.

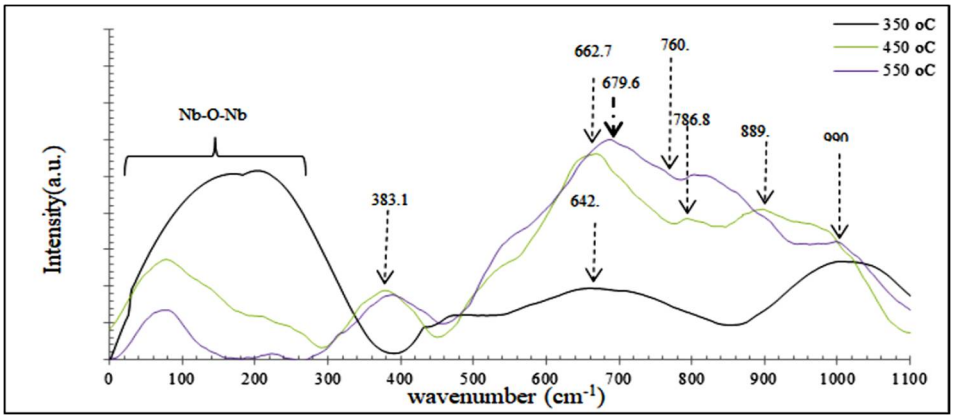

Figure 6: Raman spectra for Nb_2O_5 prepared films by Nd:YAG at different substrate temperatures

The low wavenumber region showed a lower intensity of Nb_2O_5 thin film prepared on a substrate with a temperature elevated to 550°C than Nb_2O_5 thin film prepared at 450 °C, indicating that the octahedral stretching bands were weak. Although the higher wavenumber region (> 500 cm^{-1}) showed slightly higher intensities, a distortion and broadening in the observed bands were noticed that Nb_2O_5 thin film prepared on a substrate with 450 °C showed more defined peaks. Therefore, nb_2O_5 thin film prepared at 450 °C was selected for the next step to investigate the wavelength impact on Raman scattering.

3.3 Q-Switched ND:YAG Pulsed Laser: Second Harmonic Wavelength Impact

Niobium pentoxide thin film prepared by the fundamental of Nd:YAG laser was kept for comparison. As illustrated in Figure 7, bands in the wavenumber region lower than 400 cm^{-1} are normally observed in metal oxides. A bending band was weakly observed at 291 cm^{-1} wavenumber region for thin films prepared by both wavelengths indicating Nb_2O_5 monoclinic (H-Nb_2O_5) as confirmed by ref [19]. The bands observed at 645.7 cm^{-1} were assigned for the orthorhombic structure of Nb_2O_5 thin film synthesized by 532 nm. The octahedra distortion results in shared-edge and corner-edge. The more intense scattering is assigned

for the edge-shared octahedra than the corner-shared octahedra. Thus, it can be estimated that the band that appeared in 1016 cm^{-1} was assigned for the shared-edge octahedra rather than the corner-shared octahedra. Broader bands were observed for the thin film synthesized by 532 nm wavelength may be attributed to smaller obtained particles with more dislocation densities. For further illustration, in Nb_2O_5 thin films prepared by 532 nm, the particles were smaller than in Nb_2O_5 thin films prepared by 1064 nm due to the higher energy of the shorter wavelength (532nm) being absorbed by the electronic states of the target material. This leads to the easier ejection of the energetic particles exposed to the fragmentation when a collision occurs among them pre-depositing on the substrate surface. The particle sizes were 61.6 and 42.8 nm for Nb2O5 thin films prepared by 1064 and 532 nm, respectively. As in XRD analyses, the nanoparticle dimension significantly impacts the bands that smaller particles can induce more dislocation densities within the crystal lattice planes. The molecular vibrations caused a broadening in the appearing bands' widths.

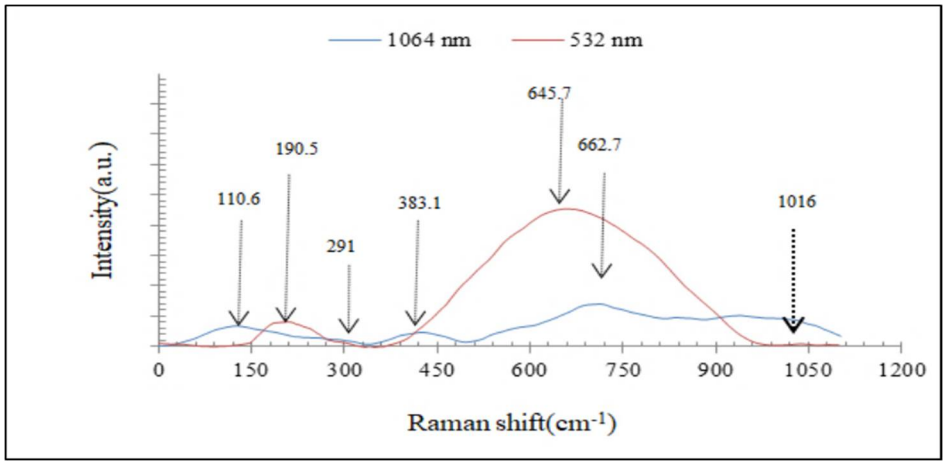

Figure 7: Raman spectra for Nb_2O_5 prepared films by Nd:YAG laser at 532 nm wavelength in comparison with 1064 nm prepared film

In addition, the phonon confinement [25] phenomenon explains the relation between the particle size (ΔX) and the phonon momentum (ΔP) that are based Heisenberg uncertainty principle as in the following equation [26-30]:

$$\Delta X \, \Delta P = \hbar^2/_4 \qquad (2)$$

Where (ħ) is the reduced Planck's constant. A smaller particle size generally leads to more confined phonons, hence increasing phonon momentum distribution. As the momentums should be conserved, the scattered phonons cause broadening in the observed Raman scattered bands.

The film prepared at 532 nm Raman behavior showed more intense and clear bands. As the particle size of Nb_2O_5 thin film prepared by 532 nm Nd:YAG laser wavelength decreased, RMS surface roughness increased slightly. As the rough texture may induce a higher scattering phenomenon, Raman observed bands showed enhanced intensities. Nb_2O_5 thin film was prepared by employing the fundamental wavelength and was still interesting to be investigated. Fixing the other parameters and changing the number of laser shots was the following step to investigate the impact of film thickness on the Raman scattering phenomenon on nanostructures.

3.4 Number of Laser Shots Impact

Raman analyses of the obtained films are shown in Figure 8. The vibrational stretching mode with a band that emerged at 308.8 cm^{-1} for the film formed by 100 pulses was indicated for the Nb-O-Nb deformed angle. A similar band assignment was found in ref [24]. However, increasing the number of laser shots with the thin film thickness caused shifting to higher values of 319.4 and 365.4 cm^{-1} for thin films prepared by 200 and 300 laser shots, respectively. This can be a result of the smaller particles of Nb_2O_5 thin film prepared via 200 laser shots that induced a phonon-electron interaction to the lower wavenumber region [31] as compared with the higher obtained thin film thickness prepared by 300 laser pulses that led to larger particle size and shifting to a higher wavenumber in this region. The prepared films' orthorhombic (T-Nb2O5) asymmetric strecthed peaks by 100, 200, and 300 laser shots were observed at 608.3, 662.7, and 494.8 cm^{-1}, respectively[19-21]. The bands at around 882.7 cm^{-1} were related to the monoclinic (H-Nb_2O_5) for thin film prepared by 100 and 200 laser pulses with enhanced intensity for the latter. Other bands for monoclinic (H-Nb_2O_5) were observed at 993 cm^{-1}. These results were agreed with ref.[18-20]. A higher intense shifted band for (H-Nb_2O_5) emerged from the thin film prepared by 300 laser shots assigned at 993.4 cm^{-1} and showed a well-agreement with the results obtained by the work in ref.[20]. This can result from enhanced crystallinity as the thin film thickness increases, leading to lower defects, including lower oxygen vacancies, dislocation densities, and microstrains. In addition, monoclinic (H-Nb_2O_5) is commonly known as the most thermodynamic stable form of Nb_2O_5 structures [5], which may result in an enhanced compression of Nb_2O_5 molecular vibrational modes.

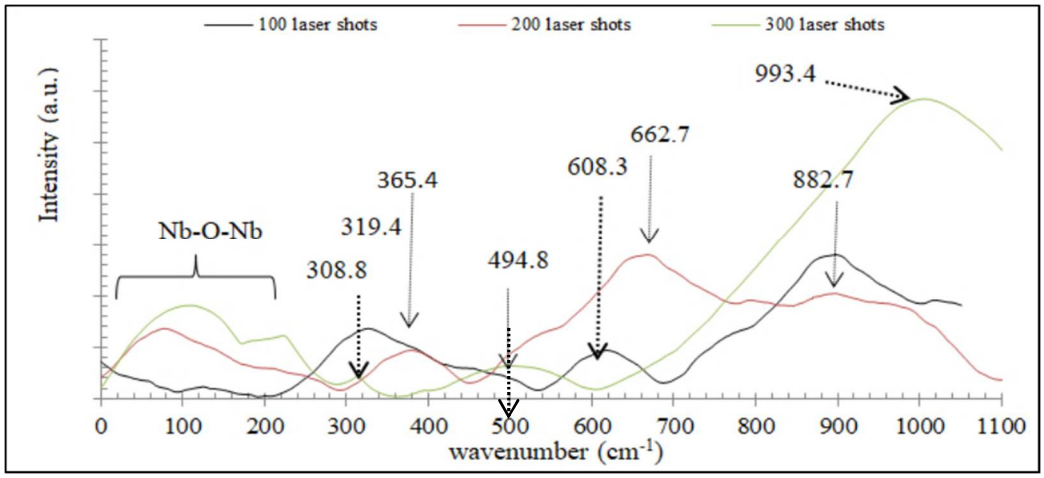

Figure 8: Raman spectra for Nb_2O_5 prepared films by Nd:YAG pulsed laser prepared film at 1064 nm and different number of laser pulses

To demonstrate the obtained results of Raman spectra, XRD analysis was required for that purpose, as shown in Figure 9. The Nb2O5 thin film sample XRD analysis was selected under the fundamental wavelength of Nd:YAG pulsed laser with 657 mJ pulse energy, 350 °C heated substrate, and 200 laser shots. The obtained diffraction peaks of polycrystalline Niobuim (v) oxides provided the orthorhombic (T-Nb_2O_5) and the monoclinic (H-Nb_2O_5) structures. These results were matched and well-agreed with the JCPDS cards' No. (00-030-0873) and (00-009-0372), respectively. Obviously, Raman spectra and the XRD profile of the prepared sample were well-agreed with the obtained diffraction peaks of Nb_2O_5 thin film. Raman spectra, as compared with the XRD pattern, can lead to a better understanding of the exact molecular structure obtained.

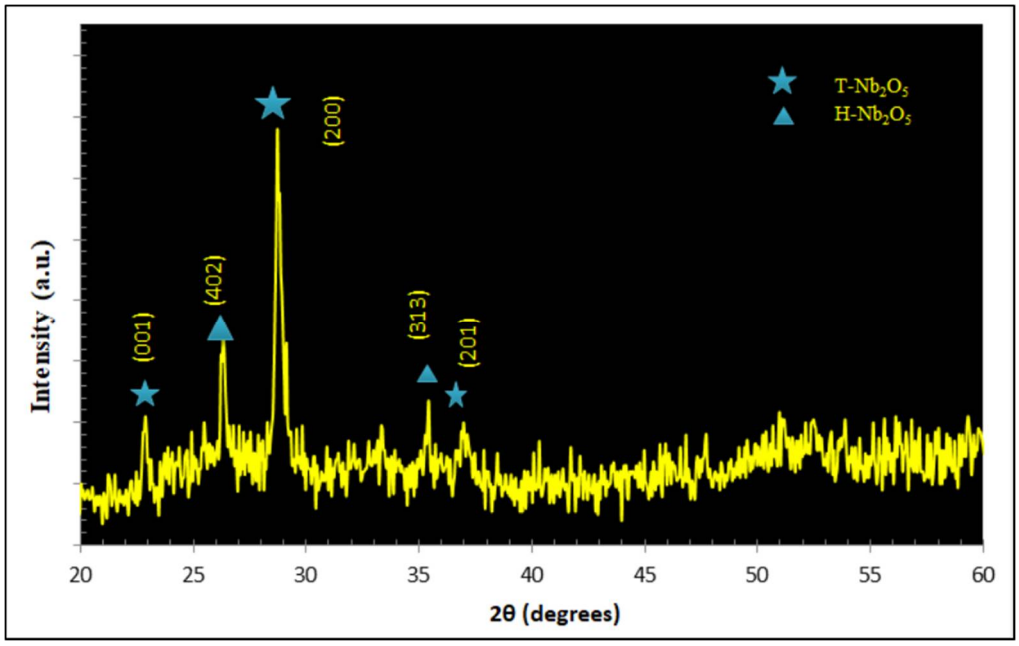

Figure 9: XRD diffraction peak profile of Nb_2O_5 sample prepared at 657 mJ energy per pulse, 350 °C, 200 laser pulses illustrating (T-Nb_2O_5) and (H-Nb_2O_5)

4. Conclusions

Raman spectra were observed and tested for Nb_2O_5 thin films prepared on quartz substrates via pulsed laser deposition under different parameters. From each parameter, a single value was selected to be fixed for the investigation of another parameter. Prepared niobium pentoxide thin films by changing the laser pulse energy showed well-organized patterns with slightly shifted values compared to previous results. The laser pulse energy of 657 mJ was selected and fixed to investigate the substrate temperature impact. Thin films synthesized by elevating the substrate temperature from 350 to 450 and then to 550 °C were tested by Raman spectroscopy. The results showed that increasing the substrate temperature led to higher intensities with slight shifting. Nb_2O_5 thin film prepared at 450 °C was selected since it showed a considerable difference from the film prepared at 350 °C and close behavior to the film prepared at 550 °C with better-defined bands. Nb_2O_5 thin films prepared by Q-switched Nd:YAG pulsed laser with a second harmonic wavelength (532 nm) were also investigated. The result showed a highly intense band around 600 cm-1 that indicated the orthorhombic (T-Nb_2O_5) structure predominance. The number of laser pulses was also

tested by the Raman scattering phenomenon to investigate the thickness impact. The results showed shifted values to higher or lower wavenumber regions due to the film's thickness, film layer arrangement, and particle size. The obtained structures were confirmed by XRD analyses.

Author contribution

All authors contributed equally to this work.

Funding

This research received no specific grant from any funding agency in the public, commercial, or not-for-profit sectors.

Data availability statement

The data that support the findings of this study are available on request from the corresponding author.

Conflicts of interest

The authors declare that there is no conflict of interest.

References

[1] N. C. Emeka, P. E. Imoisili, T. C. Jen, Preparation and characterization of nbxoy thin films: A review, Coatings, 10 (2020) 1246. https://doi.org/10.3390/coatings10121246

[2] G. RobáLee, Electrochromic Nb 2 O 5 and Nb 2 O 5/silicone composite thin films prepared by sol–gel processing, J. Mater. Chem., 1 (1991) 381–386. https://doi.org/10.1039/JM9910100381

[3] M. A. Aegerter, M. Schmitt, Y. Guo, Sol-gel niobium pentoxide coatings: Applications to photovoltaic energy conversion and electrochromism, Int. J. Photoenergy, 4 (2002) 1–10. https://doi.org/10.1155/S1110662X02000016

[4] R. Ghosh et al., Nanoforest Nb2O5 photoanodes for dye-sensitized solar cells by pulsed laser deposition, ACS Appl. Mater. Interfaces, 3 (2011) 3929–3935. https://doi.org/10.1021/am200805x

[5] R. A. Rani, A. S. Zoolfakar, A. P. O'Mullane, M. W. Austin, & K. Kalantar-Zadeh, Thin films and nanostructures of niobium pentoxide: fundamental properties, synthesis methods and applications, J. Mater. Chem. A , 2 (2014) 15683-15703. https://doi.org/10.1039/C4TA02561J

[6] S. R. Shafeeq, M. J. Abdul Razzaq, E. T. Salim, M. H. Wahid, Significance of Niobium (V) Oxide for Practical Applications: A Review,Key Eng. Mater. , 911 (2022) 89-95. https://doi.org/10.4028/p-oylf5b

[7] Eason, R. Pulsed laser deposition of thin films: applications-led growth of functional materials,John Wiley & Sons, 2007.

[8] G. Abstreiter, E. Bauser, A. Fischer, K. Ploog, Raman spectroscopy—A versatile tool for characterization of thin films and heterostructures of GaAs and AlxGa1− xAs, Appl. Phys., 16 (1978) 345–352. https://doi.org/10.1007/BF00885858

[9] S. Kawata, T. Ichimura, A. Taguchi, Y. Kumamoto, Nano-Raman scattering microscopy: resolution and enhancement, Chem. Rev., 117 (2017) 4983–5001. https://doi.org/10.1021/acs.chemrev.6b00560

[10] Varnes , A. W. and Settle, F. A. Inductively coupled plasma mass spectrometry, Handb. Instrum. Tech. Anal. Chem. Up. Saddle River, New Jersey, Prentice Hall, 1997.

[11] Skoog, D. A. Principles of instrumental analysis. Cengage learning, 2017.

[12] N. K. Hassan, M. A Fakhri, E. T Salim, Physical Properties of Pure Gold Nanoparticles and Gold Doped ZnO Nanoparticles Using Laser Ablation in Liquid For Sensor Applications, Eng. Technol. J., 40 (2022) 422-427. https://doi.org/10.30684/etj.v40i2.2242

[13] E. T. Al Waisy, M. S. Al Wazny, Responsivity, Rise Time for Bi2O3/Si Photo Detector, Eng. Technol. J., 32 (2014) 33-38.

[14] E.T .Salem, F.A. Mohamed, Transparent Oxide MgO Thin Films Prepanred By Reactive Pused Laser Deposition, Eng. Technol. J., 28 (2010) 723-730.

[15] H. A. A Abdul Amir, M. A Fakhri, A.A. Alwahib, Synthesized of GaN Nanostructure Using 1064 nm Laser Wavelength by Pulsed Laser Ablation in Liquid, Eng. Technol. J., 4 (2022) 404-411. https://doi.org/10.30684/etj.v40i2.2271

[16] H. Schäfer, R. Gruehn, F. Schulte, The modifications of niobium pentoxide, Angew. Chemie Int. Ed., 5 (1966) 40–52. https://doi.org/10.1002/anie.196600401

[17] Y. Zhao, X. Zhou, L. Ye, S. Chi Edman Tsang, Nanostructured Nb2O5 catalysts, Nano Rev., 3 (2012) 17631. https://doi.org/10.3402/nano.v3i0.17631

[18] M. R. Joya, J. J. Barba Ortega, A. M. Raba Paez, J. G. da Silva Filho, P. D. T. Cavalcante Freire, Synthesis and characterization of nano-particles of niobium pentoxide with orthorhombic symmetry, Metals, 7 (2017) 142. https://doi.org/10.3390/met7040142

[19] Z. Guan et al., Pressure induced transformation and subsequent amorphization of monoclinic Nb2O5 and its effect on optical properties, J. Phys. Condens. Matter, 31 (2019) 105401. https://doi.org/10.1088/1361-648x/aaf9bd

[20] F. D. Hardcastle, I. E. Wachs, Determination of niobium-oxygen bond distances and bond orders by Raman spectroscopy, Solid State Ion., 45 (1991) 201–213. https://doi.org/10.1016/0167-2738(91)90153-3

[21] K. Skrodczky et al., Niobium pentoxide nanomaterials with distorted structures as efficient acid catalysts, Commun. Chem., 2 (2019) 129. https://doi.org/10.1038/s42004-019-0231-3

[22] X. Wang et al., Temperature dependence of Raman scattering in β-(AlGa) 2O3 thin films, AIP Adv., 6 (2016) 15111. https://doi.org/10.1063/1.4940763

[23] N. Usha, R. Sivakumar, C. Sanjeeviraja, M. Arivanandhan, Niobium pentoxide (Nb2O5) thin films: rf Power and substrate temperature induced changes in physical properties, Optik - Int. J. Light and Electron. Opt.,126 (2015) 1945–1950. https://doi.org/10.1016/j.ijleo.2015.05.036

[24] A. M. Raba, J. Bautista-Ruíz, M. R. Joya, Synthesis and structural properties of niobium pentoxide powders: A comparative study of the growth process, Mater. Res., 19 (2016) 1381–1387. https://doi.org/10.1590/1980-5373-MR-2015-0733

[25] H. C. Choi, Y. M. Jung, S. Bin Kim, Size effects in the Raman spectra of TiO2 nanoparticles, Vib. Spectrosc., 37 (2005) 33–38. https://doi.org/10.1016/j.vibspec.2004.05.006

[26] R. A Ismail, E. T Salim, H. T Halbos, Preparation of Nb2O5 nanoflakes by hydrothermal route for photodetection applications: The role of deposition time, Optik, 245 (2021) 167778. https://doi.org/10.1016/j.ijleo.2021.167778

[27] M. A Fakhri, F. G Khalid, E. T Salim, Influence of annealing temperatures on Nb2O5 nanostructures prepared using Pulsed Laser Deposition method, J. Phys. Conf. Ser.,1795, 2021, 012063. http://dx.doi.org/10.1088/1742-6596/1795/1/012063

[28] E. T. Salim, J. A Saimon, M. K Abood, M. A Fakhri, Electrical conductivity inversion for Nb2O5 nanostructure thin films at different temperatures, Mater. Res. Express, 6 (2020) 126459. https://doi.org/10.1088/2053-1591/ab771c

[29] E.T Salim, J. A Saimon, M. K Abood, M. A Fakhri, Effect of silicon substrate type on Nb2O5/Si device performance: an answer depends on physical analysis, Opt. Quantum Electron., 52 (2020) 463. https://doi.org/10.1007/s11082-020-02588-y

[30] E. K. Hamed, M. A .Fakhry , F. A. Hattab, Laser Energy Effects on Optical Properties of Titanium Di-Oxide Prepared by Reactive Pulsed Laser Deposition, Eng. Technol. J., 30 (2012) 3104-3111.

[31] M. V. V. Prasad, K. Thyagarajan, B. R. Kumar, Effect of annealing temperature on structural and Raman spectroscopy analysis of nanostructured CdS thin films, IOP Conf. Ser.Mater. Sci. Eng., 149 (2016) 012051. https://doi.org/10.1088/1757-899X/149/1/012051